International Journal of Engineering

Journal Homepage: www.ije.ir

Design of a Circular Patch Antenna with Parasitic Elements for 5G Applications

S. Lamultree*[a], M. Phalla[a], P. Kunkritthanachai[a], C. Phongcharoenpanich[b]

[a] *Faculty of Engineering, Rajamangala University of Technology Isan Khonkaen Campus, Khonkaen, Thailand*
[b] *School of Engineering, King Mongkut's Institute of Technology Ladkrabang, Bangkok, Thailand*

P A P E R I N F O

Paper history:
Received 20 May 2023
Received in revised form 26 June 2023
Accepted 09 July 2023

Keywords:
Circular Patch Antenna
Wideband Antenna
Parasitic Elements
5G Applications

A B S T R A C T

A design of a wideband bidirectional pattern antenna, accomplished by the integration of a circular patch, crescents as parasitic elements, encompassed by a circular ring adjoining the ground plane, to operate over the mid-band 5G sub-6 GHz applications is reported. It is come up with a copper grazed on FR4 substrate with relative permittivity of 4.3 and height of 1.6 mm. The proposed antenna is fed by a 50-ohm coplanar waveguide, which is printed on the same side of the radiating circular patch. A concise antenna model with dimensions of 45 × 45 × 0.6 mm^3 was made up and investigated to affirm the simulation outcomes. Good consistency was confirmed between experimental and simulation results. The proposed antenna has the benefit of bidirectional pattern with a good gain of 5.24 dBi and wide bandwidth covering of 111.4% (1.81-6.36 GHz) — it is one of good postulants for 5G new radiation application especially for indoor environment, narrow, and long path services area like corridor, tunnel, and train station, etc.

***doi**: 10.5829/ije.2023.36.09c.13*

Graphical Abstract

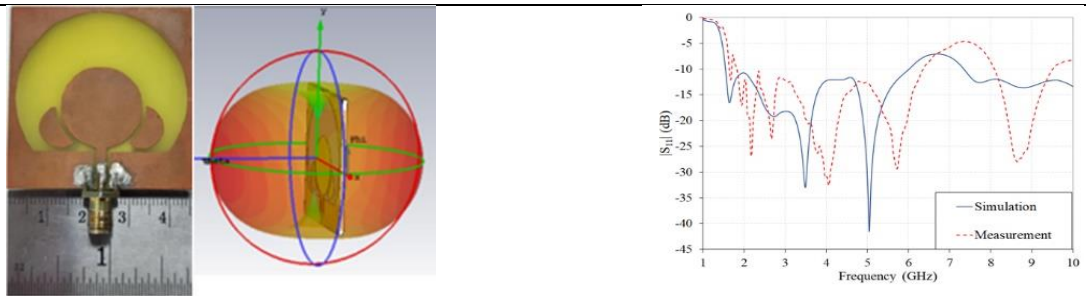

NOMENCLATURE

w	width of the substrate	h	thickness of the substrate
l	length of the substrate	CR	circular ring
r_1	radius of the circular patch	CPW	coplanar waveguide
r_2	radius of the enforced-radiation circular ring	CWBPA	compact wideband bidirectional pattern antenna
r_m	radius of the crescent	DGS	defected ground structure
g_2	gap between the radiating circular patch and crescent	FBW	fractional bandwidth
s	space between the crescent and ground plane	GND	ground plane
t	thickness of copper layer	IBW	impedance bandwidth
l_f	length of feeding strip	RCP	radiating circular patch
w_f	width of feeding strip	RLBW	return loss bandwidth
l_g	length of ground plane	NR	new radio
g	gap between feed line and ground plane	UWB	ultra-wideband

*Corresponding Author Email: suthasinee.la@rmuti.ac.th (S. Lamultree)

Please cite this article as: S. Lamultree, M. Phalla, P. Kunkritthanachai, C. Phongcharoenpanich, Design of a Circular Patch Antenna with Parasitic Elements for 5G Applications, ***International Journal of Engineering, Transactions C: Aspects***, Vol. 36, No. 09, (2023), 1686-1694

1. INTRODUCTION

With the swift enlargement of fifth generation (5G) and beyond wireless networks and exploitation of higher data transmission rates, increasing provocations have been resulted in advocate a large scale of ultramodern utility frameworks and utilizations with high reliability, low latency, lately [1, 2]. One of the 5G plans is to employ the sub-6 GHz band — n34(2010–2025 MHz), n38 (2570–2620 MHz), n40 (2300–2400 MHz), n41 (2496–2690 MHz), n46 (5150–5925 MHz), n77 (3300–4200 MHz), n79 (4400–5000 MHz), etc. — which, also covered mid-band of 5G (2 to 6 GHz), leading high data rates, huge capacity as well as good coverage from the essential number of available spectrums [3, 4]. Modern wireless communications stretch out to new standard applications, algorithms, propagation techniques [5, 6], vigorous hardware defiance as well as the relevant antenna design [7-10] fulfilling human needs. As the performance of the antenna results considerable influence on the accomplishment of the plenary communication systems. Lately, research on 5G antenna is very attractive and has been a continuing process [11-13]. For literal applications, the extensively utilized compact size and broadband antennas are more delightful [14-20]. Since, wideband antennas are a good advancement in the 5G new radiation (NR) applications and upcoming generations of wireless communication systems, as it would handle at widen frequency extend accordingly receding the use of miscellaneous antennas in a single device shrinking the mutual coupling and intervention in the system as well as economizing financial plan.

Massive wideband antennas were conducted and developed continuously over the past decade with multitudinous techniques [21-25]. To improve the impedance bandwidth (IBW), different shapes of main radiator had been modified as well as the ground plane (GND) structures [14, 18, 25]. Ghobadi, and Majidzadeh [14] presented the ultra-wideband (UWB) antenna that printed on FR4 substrate and operated over 2.9-16 GHz by applying a semi-circle-shaped-slot cutting from the GND to improve IBW. A microstrip-fed printed monopole antenna for super wide band antenna was introduced by Balani et al. [18] to obtain wide bandwidth, the main radiating patch had been modified by adjoining a pair of ears at the upper part of the radiator as well as modifying its partial GND, making its geometry complexity. With super wide IBW, the stabilized radiation properties with less distortion mainly at higher frequency could not avoid. Koma'rudin et al. [25] presented the staircase-shaped steps adding to the bottom section of the main radiator patch to ameliorate the IBW; however, the antenna geometry was more complicated gathering with the multi-layers structure. Varamini et al. [16] and Wang et al. [22] presented metasurface techniques to make the widen bandwidth and antenna gain. Even though the planar scales of metasurface antennas are normally bulky, stint its utilization. Asmeida et al. [23] introduced the combination of adding different shapes of slot on the radiator and defected ground structure (DGS) to improve the IBW of 74.6% as well as preserve the polarity bandwidth. In addition, others possible techniques for refining the bandwidth of the antenna were implemented — the complexity of fractal structure [16, 21, 24], adding slots [17, 19], the stubs and addition elements of modified radiators [18, 20, 23], and parasitic loading [4, 15, 24], so on. Others in demand method to grant an expedient matching tuning mechanism by using balun and coupled feed was realized by Ta et al. [7] and Asmeida et al. [23]. Notwithstanding, the compactness and wideband coverage antenna for the 5G NR and upcoming generation wireless terminal stands still demand in taking steps forward the proportions and radiation properties to be stable.

This article, a study and design of a compact wideband bidirectional pattern antenna (CWBPA) for mid-band of 5G applications operated frequency ranging from 2 to 6 GHz which included the sub-6 GHz is proffered. The profit of this presented antenna is that the concise size, facile fabric, and bidirectional pattern operating over wide bandwidth. With these advantages, thereby, the proposed antenna is one of good selectness for 5G application—installing as the antenna at the base station especially along the narrow and long path service propagation areas like corridor, tunnel, train station and so on. The resultant of the supplemented elements of antenna fabrication will be analyzed and evaluated. In the study, the pivotal preliminary parameters are reckoned by using the formulas in section 2. From those parameters, simulation was kept on operated by CST microwave studio [26] to numerically discover the final set of parameters. Numerical and substantiation results are revealed thoroughly.

2. THE RATIONALE OF ANTENNA DESIGN

This section narrates the construction of the evolved antenna and the reasoning to the rear of using a pair of crescents in the design. In the design process, the coplanar waveguide (CPW) fed circular patch (Ant #1) was considered in the beginning. It comprised of a radiating circular patch (RCP) of radius r_1 printed on top of an FR4 substrate of the width w (a value 45 mm), the substrate length l (a value 45 mm) and fed by a 50-Ω CPW of GND length l_g, fed line width w_f, fed line length l_f and gap between feed line and GND g as shown in Figure 1(a). The Ant #1 provided an omnidirectional pattern with wide IBW (3.08-10 GHz) as depicted in Figures 2 (a) and 3. Subsequently, Ant #2 was formed by adding a circular ring (CR) of radius r_2 extending the

GND, as shown in Figure 1(b), to impose the radiation pattern propagating in forward and backward directions as plotted in Figure 2(b). An unintentional sake of this CR was that it also leashed the 10 dB return loss bandwidth (RLBW) to be widened (covered 1.8 to 9 GHz) and tended to be dual band since the $|S_{11}|$ around 4.8 GHz was worsened as shown in Figure 3. At this stage, a 10 dB RLBW covering the interested frequency band ranging from 2 to 6 GHz was uncompleted. The final stage of completing the CWBPA, a pair of crescents of radius r_m was gathered in the structure as parasitic elements beside the RCP with the gap g_2 of 1 mm as shown in Figure 1(c). Consequently, the 10 dB RLBW over the interested frequency band as well as the bidirectional pattern was achieved as shown in Figures 2(c) and 3.

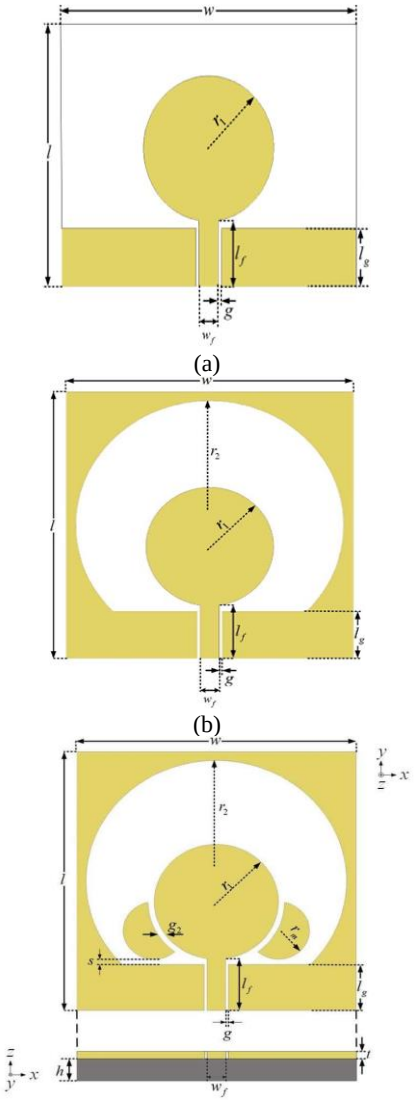

Figure 1. The structure of the developed antenna: (a) Ant #1 (b) Ant #2 and (c) proposed antenna

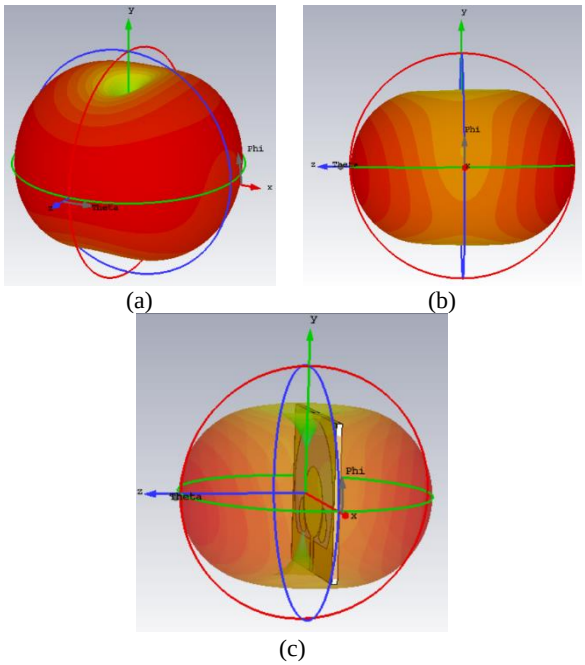

Figure 2. 3D radiation pattern of: (a) Ant #1 (b) Ant #2 and (c) proposed antenna

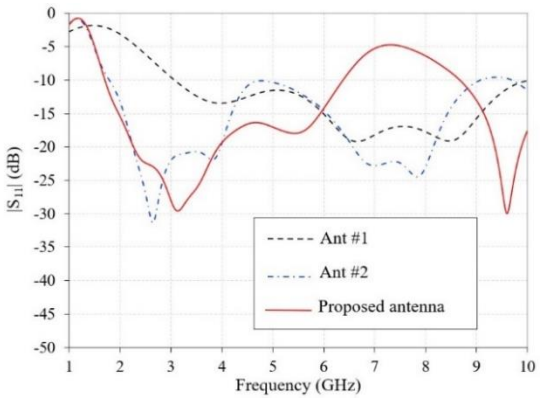

Figure 3. Comparing $|S_{11}|$ among three antennas

Based on the ensuing formulas, the initial parameters of the presented antenna are calculated and assigned [27].

$$r = \frac{F}{\left\{1+\frac{2h}{\pi\varepsilon_r F}\left[\ln\left(\frac{\pi F}{2h}\right)+1.7726\right]\right\}^{1/2}} \quad (1)$$

where, F is a function of resonant frequency for the dominant mode of TE_{11} as shown in Equation (2)

$$F = \frac{8.791\times10^9}{f_r\sqrt{\varepsilon_r}} \quad (2)$$

r is referred to the design radius of the RCP of r_1 and an CR of radius r_2; ε_r is the relative permittivity of the FR4 substrate of 4.3; h is the thickness of the substate of 0.16

cm. Note that the unit of h in Equation (1) is in cm. f_r is a resonant frequency—the radius of RCP of r_1 is designed to resonate 4 GHz while the radius of CR of r_2 is designed for f_r of 2 GHz. Considering the fringing effect in the above formulas, the initial r_1 of 10 mm and r_2 of 21 mm are come by, respectively. For the strip line of 50-Ω impedance matching, the width w_f and length l_f of feed line are computed by Equations (3)-(5) [27]:

$$\frac{w_f}{h}=\frac{2}{\pi}\left[\begin{array}{l}B-1-\ln(2B-1)\\+\frac{\varepsilon_r-1}{2\varepsilon_r}\left\{\ln(B-1)+0.39-\frac{0.61}{\varepsilon_r}\right\}\end{array}\right] \quad (3)$$

where $B=60\pi^2(Z_o\sqrt{\varepsilon_r})^{-1}$ and Z_0 is the characteristic impedance of 50 Ω.

$$l_f=\lambda/4\sqrt{\varepsilon_{eff}} \quad (4)$$

where ε_{reff} is the effective dielectric constant of the substrate.

$$\varepsilon_{reff}=\frac{\varepsilon_r+1}{2}+\frac{\varepsilon_r-1}{2}\sqrt{1+\frac{12h}{w_f}} \quad (5)$$

For the gap g between feed line and GND of CPW, it is related the 50-ohm impedance Z_0 in Equation (6) [28]:

$$Z_0=30\pi K'(k)/\sqrt{\varepsilon_{eff}}K(k) \quad (6)$$

where $K(k)$ and $K'(k)$ are the complete elliptic integral of the first kind

$$K(k)=\int_0^{\phi}\frac{d\theta}{\sqrt{1-k^2\sin^2\theta}},\begin{cases}0\le k^2<1\\0\le\phi<\frac{\pi}{2}\end{cases} \quad (7)$$

$$K'(k)=K(k')=\sqrt{1-k^2} \quad (8)$$

where the ratio of $K(k)/K'(k)$ and k is defined as follows:

$$\frac{K(k)}{K'(k)}=\begin{cases}\frac{\pi}{\ln[2(1+\sqrt{k'})/(1-\sqrt{k'})]}, & 0\le k\le 0.707\\\frac{1}{\pi}\ln[2(1+\sqrt{k})/(1-\sqrt{k})], & 0.707\le k\le 1\end{cases} \quad (9)$$

and

$$k=w_f/(2g+w_f) \quad (10)$$

As the results, the w_f of 3 mm, l_f of 10 mm and g of 0.45 mm are assigned throughout the report. Note that the length of GND below the RCP of lg is 9 mm.

Moreover, the radius r_m of the crescent beside the RCP is as initially calculated by Equation (11) [29]:

$$r_m=\frac{72-sf_m}{2.25f_m} \quad (11)$$

where f_m is the design frequency (the unit of f_m in Equation (11) is in GHz), and s is the spacing between the crescent and GND (the value of 1 mm) and the unit of r_m is in mm.—this work the radius r_m is designed at the frequency of 4.8 GHz, therefore, the initial r_m is 6 mm.

All satisfactory parameters are acquired using the CST simulation and sorted in Table 1. To confirm the simulation outcome, a prototype of CWBPA is made up following the designed dimensions in Table 1 as shown in Figure 4. The CWBPA prototype is soldered to a 50-ohm SMA connector for extending to a coaxial feed line. The $|S_{11}|$, 2D radiation patterns and antenna gain of the presented CWBPA are evaluated and demonstrated by using E5063A network analyzer.

3. RESULTS AND DISCUSSION

The simulation and measured results of the proposed CWBPA are exposed in this section. In the simulation process, the SMA connector excludes the antenna model to focus on only antenna properties. However, the antenna model with SMA is considered in the final stage. From the developed CWBPA by adding a pair of crescents in the previous section, the radius rm, gap between patch g2 and the spacing s are demonstrated.

TABLE 1. Selected best values for parameters of the CWBPA

Parameter	Value (mm)	Parameter	Value (mm)
w	45	t	0.035
l	45	l_f	10
r_1	10	w_f	3
r_2	21	l_g	9
r_m	5	g	0.45
g_2	1	h	1.6
s	1		

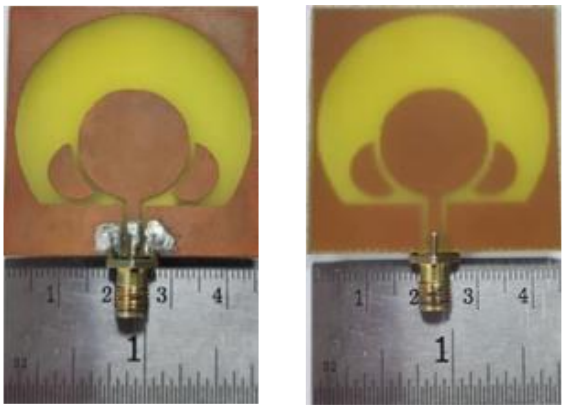

(a) (b)

Figure 4. CWBPA prototype: (a) front view, (b) rear view

The effect of r_m on $|S_{11}|$ is considered by varying r_m 3 to 7 mm as plotted in Figure 5. Noticeably, the larger radius, as the narrower 10 dB RLBW is attained. For the compelling frequency band ranging from 2 to 6 GHz for mid-band 5G, the smaller r_m offers the $|S_{11}|$ worsened around 4.8 GHz, while the r_m of 6 and 7 mm cannot offer the 10 dB return loss over the considering band. This work, the radius r_m of 5 mm is selected because it proffers a good $|S_{11}|$ over the considering frequency band.

Moreover, the varying gab g_2 between the crescent and the RCP of values 0, 1 and 2 mm is also studied on its effect to the $|S_{11}|$ as shown in Figure 6. Obviously, the $|S_{11}|$ is worsened when the crescent adjoins the RCP (g_2= 0) — it provides the narrow RLBW covering 1.7 to 2.54 GHz and 4.43 to 5.05 GHz. The larger gab g_2 yields the wider 10 dB RLBW — for the g_2 of 1, and 2 mm, it covers the frequency ranging from 1.71 to 6.38 GHz, and 1.72 to 6.43 GHz, respectively. Nonetheless, focusing on the interesting frequency band (2 to 6 GHz), g_2 of 1 mm furnishes the overall trend of $|S_{11}|$ better than the value 2 mm since g_2 of 2 mm offers the $|S_{11}|$ near the value -10 dB at 4.5 GHz. For that reason, the g_2 of 1 mm is selected. Additionally, the influence of the space between the crescent and GND, s, is also considered by varying the spacing s of 1, 3 and 6 mm as depicted in Figure 7. The further the spacing s as the wider 10 dB RLBW is achieved, contrast to the worsen $|S_{11}|$ occurrence around 4.5 GHz. Among these three different values, the spacing s of 1 mm impacts on the excellent $|S_{11}|$ over the interesting frequency band. Accordingly, the spacing s of 1 mm is chosen. Therefore, the CWBPA is achieved with the 10 dB RLBW of 1.71–6.38 GHz. At the final stage of the design, for the interested band (2 to 6 GHz), the proposed CWBPA comes up with the total efficiency of more than 81.7%, the minimum and maximum simulated gains of 2.63 dBi and 5.55 dBi and minimum and maximum measured gains of 2.33 dBi and 5.24 dBi, respectively as shown in Figure 8.

To affirm the simulation, the experimental process of testing $|S_{11}|$ and radiation pattern of the developed CWBPA is set up. Figure 9 exhibits the numerical and experimental $|S_{11}|$ for various frequency ranging from 1 GHz to 10 GHz. Visibly, the measured $|S_{11}|$ are reasonably in nice agreement the simulation results covering the 10 dB RLBW over the mid-band of 5G applications — the measured $|S_{11}|$ is 1.81–6.36 GHz covered the fractional bandwidth (FBW) of 111.4% and

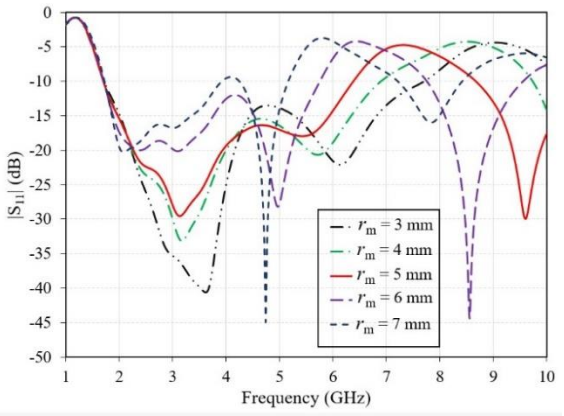

Figure 5. $|S_{11}|$ for various r_m

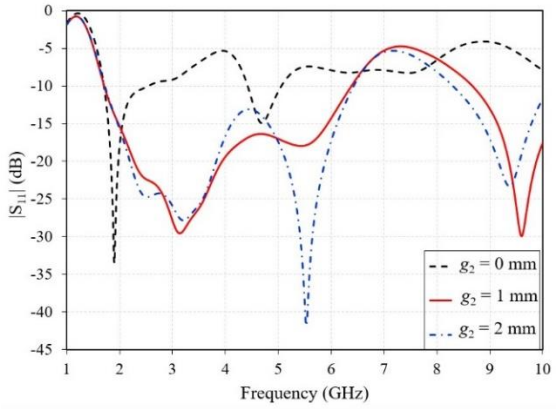

Figure 6. $|S_{11}|$ for various g_2

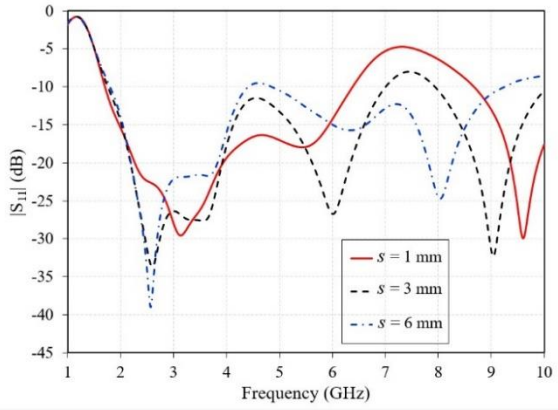

Figure 7. $|S_{11}|$ for various s

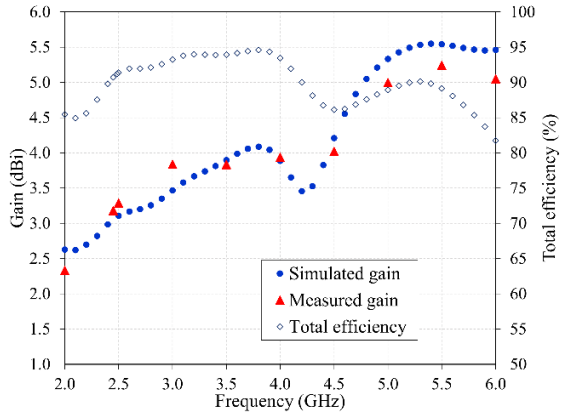

Figure 8. Gain and efficiency of the developed CWBPA

the simulation is 1.55–6.01 GHz covered the FBW of 118%. Note that the simulation in Figure 9 includes the SMA connector where with it is like the actual ambient that the antenna is connected to the cable via SMA connector.

Besides the impedance characteristics, the 2D radiation pattern in *xz*- and *yz*-planes at the frequencies of 2, 4 and 6 GHz is also examined as demonstrated in Figures 10-12. Evidently, the tested radiation patterns follow the common trend and acceptable agreement with the simulated results and the values do not deviate much from each other. The deviation is likely to be from a minor difference in the numerical and experimental setup. This proposed CWBPA yields a bidirectional pattern, linear polarization, peak simulated gains of 2.63/3.89/5.46 dBi and tested gains of 2.33/3.94/5.05 dBi at the operating frequencies of 2/4/6 GHz, respectively. In addition, the simulated and measured HPBWs in *xz*-plane are 162.6/104.3/65.2 degree and 157/88/48 degree, respectively. For *yz*-plane, the simulated and measured results are 84.4/73.3/53.4 degree and 86/62/56 degree, respectively. Note that the level of cross-polarization in *xz*-plane is less than −20 dB for all intended frequency ranges, while the high level of cross-polarization in *yz*-plane is achieved at a frequency higher than 4 GHz.

Over and above, the performance of the proposed CWBPA was bearded comparison with current compact, wideband and 5G antennas published between 2017 to 2023 as tabulated in Table 2. The antenna implemented by Paul et al. [4] using RT5880, larger dimension offering an omnidirectional pattern with lower gain covering the narrower bandwidth was proposed. The geometry of the antenna was uncomplicated. The antenna dimensions reported in literature [7, 12-13, 25] had a larger size, more complexity, provided unidirectional pattern covering narrower bandwidth. Ta et al. [7] and Saleh et al. [13] offered a higher gain, while Cai et al. [12] offered a lower gain compared to this work. The antenna offered by Koma'rudin et al. [25] fainty higher gain. The antenna implemented by Samsuzzaman and Tariqul Islam [17] using FR4 substrate, approximately the same electric proportions offering a bidirectional pattern with faintly lower gain, but it operated covering widen bandwidth. Additionally, Yazdani et al. [10] proposed the array arrangement antenna implemented by different material, larger size, provided the stable bidirectional pattern covering three different bands, narrower bandwidth, and higher gains in the second and the third bands. Another work, the smaller proportions antenna, implemented by the same material, more complicated structure, provided a bidirectional pattern with lower gain covering a narrower bandwidth was presented by Sonu et al. [20]. Asmeida et al. [23] implemented an omnidirectional pattern using different

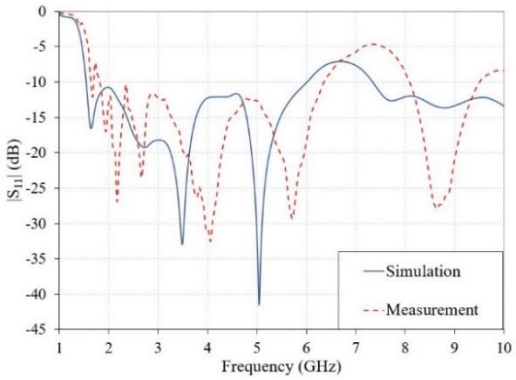

Figure 9. Simulated and measured $|S_{11}|$

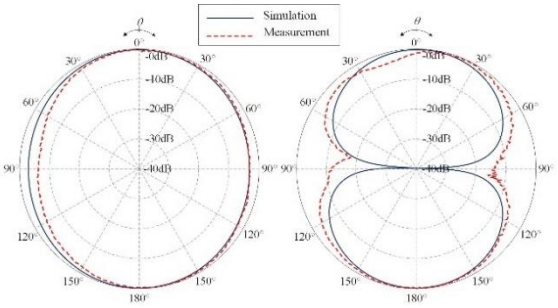

(a) (b)

Figure 10. Radiation pattern at 2 GHz: (a) *xz*-plane and (b) *yz*-plane

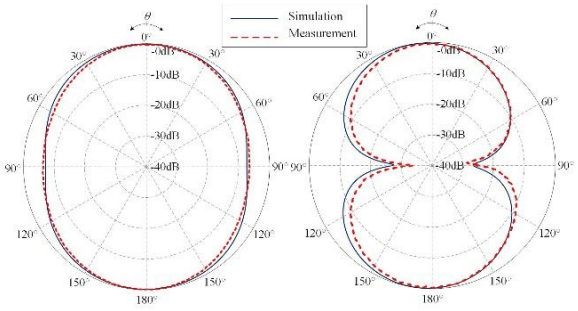

(a) (b)

Figure 11. Radiation pattern at 4 GHz: (a) *xz*-plane and (b) *yz*-plane

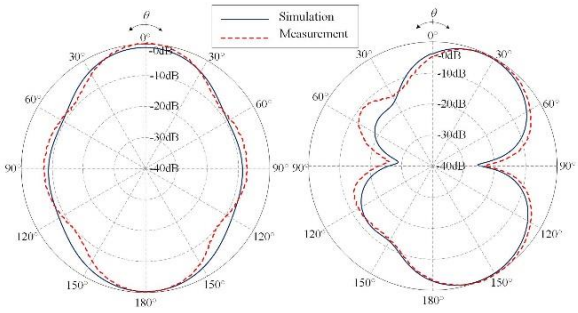

(a) (b)

Figure 12. Radiation pattern at 6 GHz: (a) *xz*-plane and (b) *yz*-plane

TABLE 2. Comparison between previous studies and this current research

Ref.	Size (λ)	Sub.	Patt.	FBW (%)	Gain (dBi)	Com.
[4]	0.36×0.36×0.01	RT 5880	Omni	44.5	3.51	L
[7]	n/a×0.87×0.02	RT 5880	Uni	36.2	5.8	M
[10]	0.31×0.28×0.002	RO 4003	Bi	9.5/21.9/12.2	1/6/10	L
[12]	1.65×0.83×0.08	FR4	Uni	35.3	3.5	H
[13]	1.07×1.07×0.61	RT 5880	Uni	21.4	12.7	H
[17]	0.29×0.29×0.01	FR4	Bi	126.85	4.85	L
[20]	0.20×0.22×0.01	FR4	Bi	61.1	3.5	M
[23]	0.28×0.35×0.08	RT 5880	Omni	74.6	3.6	L
[25]	0.66×0.76×0.01	Felt	Uni	79.8	5.51	M
This work	0.27×0.27×0.01	FR4	Bi	111.4	5.24	L

material with a slightly larger dimension, proffered a narrower bandwidth and lower gain than this proposed CWBPA. With a simple fabric, concise proportions, bidirectional pattern covered wideband transition sub-6 GHz 5G NR; thereby, this proposed CWBPA is one of the good candidates for 5G NR applications.

λ means a free-space wavelength at the lowest operated frequency; abbreviations: n/a (not applicable), Sub. (substrate of material), Patt. (pattern), Uni (unidirectional). Omni (omnidirectional), Bi (bidirectional), Com. (complexity), L (low), M (medium), H (high).

In this work, a single antenna has been studied, designed, analyzed, and illustrated its effecting in the basic antenna theory and tested in the laboratory. The 10 dB return loss, radiation pattern and gain of the single antenna have been evaluated. Nevertheless, it conveys some significant concepts for the antenna design and application.

4. CONCLUSION

A design of a CWBPA, contrived by the circular patch, circumscribed in the circular ring, incorporated with the parasitic elements beside the radiating patch, covering the sub-6 GHz 5G NR frequency band has been reported. It is printed on the top side of FR4 substrate, fed by 50-ohm CPW, and adjoined to the coaxial line via SMA connector. The key role of ameliorating the 10 dB return loss bandwidth of the presented antenna is that the pair of parasitic crescents as disclosed. This CWBPA yields the corresponding FBW of 111.4% (1.81–6.36 GHz) covering the mid-band 5G application, linearly polarized, peak gain of 5.24 dBi and the total efficiency of more than 81.7%. The experimental $|S_{11}|$, 2D radiation pattern and gain insist nifty the simulation results. With the compactness proportions, an effortless structure, bidirectional pattern accompanied by wideband operation frequency and high gain, this proposed antenna is one of good potential candidates for subbase station antenna to service at indoor environment, the long and narrow path areas like troll, train station, tunnel, sky train stations, etc.

5. ACKNOWLEDGMENTS

This research project is supported by Rajamangala University of Technology Isan. Contract No. ENG3/66.

6. REFERENCES

1. Sonkki, M., Antonino-Daviu, E., He, D. and Myllymäki, S., "Advanced simulation methods of antennas and radio propagation for 5g and beyond communications systems", ***International Journal of Antennas and Propagation***, Vol. 2020, (2020), 1-3. https://doi.org/10.1155/2020/4387494
2. Dicandia, F.A., Fonseca, N.J., Bacco, M., Mugnaini, S. and Genovesi, S., "Space-air-ground integrated 6g wireless communication networks: A review of antenna technologies and application scenarios", ***Sensors***, Vol. 22, No. 9, (2022), 3136. https://doi.org/10.3390/s22093136
3. Hussain, S., Qu, S.-W., Sharif, A.B., Abubakar, H.S., Wang, X.-H., Imran, M.A. and Abbasi, Q.H., "Current sheet antenna array and 5g: Challenges, recent trends, developments, and future directions", ***Sensors***, Vol. 22, No. 9, (2022), 3329. https://doi.org/10.3390/s22093329
4. Paul, L.C., Saha, H.K., Rani, T., Mahmud, M.Z., Roy, T.K. and Lee, W.-S., "An omni-directional wideband patch antenna with parasitic elements for sub-6 ghz band applications", ***International Journal of Antennas and Propagation***, Vol. 2022, (2022). https://doi.org/10.1155/2022/9645280
5. Firdaus, F., Fadhillah, I., Ahmad, N. and Mohd Alic, A., "A light solution for device diversity problem in a wireless local area network fingerprint indoor positioning system", ***International***

Journal of Engineering, Transaction A: Basics, Vol. 36, No. 4, (2023), 649-658. doi: 10.5829/IJE.2023.36.04A.05.

6. Sridher, T., Sarma, A. and Naveen Kumar, P., "Performance evaluation of onboard wi-fi module antennas in terms of orientation and position for iot applications", ***International Journal of Engineering, Transaction A: Basics***, Vol. 35, No. 10, (2022), 1918-1928. doi: 10.5829/IJE.2022.35.10A.11.
7. Ta, S.X., Choo, H. and Park, I., "Broadband printed-dipole antenna and its arrays for 5g applications", ***IEEE Antennas and Wireless Propagation Letters***, Vol. 16, (2017), 2183-2186. doi: 10.1109/LAWP.2017.2703850.
8. Saraereh, O.A., "A novel broadband antenna design for 5g applications", ***CMC-Comput. Mater. Continua***, Vol. 67, No. 1, (2021), 1121-1136. https://doi.org/10.32604/cmc.2021.015066
9. Patnaik, A. and Kartikeyan, M., "Compact dual and triple band antennas for 5g-iot applications", ***International Journal of Microwave and Wireless Technologies***, Vol. 14, No. 1, (2022), 115-122. https://doi.org/10.1017/S1759078721000301
10. Yazdani, R., Aliakbarian, H., Sahraei, A. and Vandenbosch, G.A., "A compact triple-band dipole array antenna for selected sub 1 ghz, 5g and wifi access point applications", ***IET Microwaves, Antennas & Propagation***, Vol. 15, No. 15, (2021), 1866-1876. https://doi.org/10.1049/mia2.12200
11. Abolade, J.O., Konditi, D.B., Mpele, P.M., Orimogunje, A.M. and Oguntoye, J.P., "Miniaturized dual-band antenna for gsm1800, wlan, and sub-6 ghz 5g portable mobile devices", ***Journal of Electrical and Computer Engineering***, Vol. 2022, (2022). doi: 10.1155/2022/5455915.
12. Cai, J., Zhang, J., Xi, S., Huang, J. and Liu, G., "A wideband eight-element antenna with high isolation for 5g new-radio applications", ***Applied Sciences***, Vol. 13, No. 1, (2022), 137. https://doi.org/10.3390/app13010137
13. Saleh, C.M., Almajali, E., Jarndal, A., Yousaf, J., Alja'Afreh, S.S. and Amaya, R.E., "Wideband 5g antenna gain enhancement using a compact single-layer millimeter wave metamaterial lens", ***IEEE Access***, Vol. 11, (2023), 14928-14942. doi: 10.1109/JSAC.1987.1146527.
14. Ghobadi, C. and Majidzadeh, M., "Multi attribute analysis of a novel compact uwb antenna with via-fed elements for dual band notch function", ***International Journal of Engineering, Transactions A: Basics***, Vol. 27, No. 10, (2014), 1565-1572. doi: 10.5829/idosi.ije.2014.27.10a.10.
15. Ding, K., Gao, C., Zhang, B., Wu, Y. and Qu, D., "A compact printed unidirectional broadband antenna with parasitic patch", ***IEEE Antennas and Wireless Propagation Letters***, Vol. 16, (2017), 2341-2344. doi: 10.1109/LAWP.2017.2718000.
16. Varamini, G., Keshtkar, A. and Naser-Moghadasi, M., "Compact and miniaturized microstrip antenna based on fractal and metamaterial loads with reconfigurable qualification", ***AEU-International Journal of Electronics and Communications***, Vol. 83, (2018), 213-221. doi: 10.1016/j.aeue.2017.08.057.
17. Samsuzzaman, M. and Islam, M.T., "Circularly polarized broadband printed antenna for wireless applications", ***Sensors***, Vol. 18, No. 12, (2018), 4261. https://doi.org/10.3390/s18124261
18. Balani, W., Sarvagya, M., Samasgikar, A., Ali, T. and Kumar, P., "Design and analysis of super wideband antenna for microwave applications", ***Sensors***, Vol. 21, No. 2, (2021), 477. https://doi.org/10.3390/s21020477
19. Qi, Z., Ding, X., Yang, W. and Chen, J., "A compact broadband planar inverted-f antenna with dual-resonant modes", ***Applied Sciences***, Vol. 12, No. 17, (2022), 8915. https://doi.org/10.3390/app12178915
20. Rana, S., Verma, J. and Gautam, A.K., "A wideband circularly polarized cpw-fed diamond shape microstrip antenna for wlan/wimax applications", ***Progress In Electromagnetics Research C***, Vol. 131, (2023), 25-33. doi: 10.2528/PIERC22122106.
21. Biswas, B., Ghatak, R. and Poddar, D., "A fern fractal leaf inspired wideband antipodal vivaldi antenna for microwave imaging system", ***IEEE Transactions on Antennas and Propagation***, Vol. 65, No. 11, (2017), 6126-6129. doi: 10.1109/TAP.2017.2748361.
22. Wang, J., Wong, H., Ji, Z. and Wu, Y., "Broadband cpw-fed aperture coupled metasurface antenna", ***IEEE Antennas and Wireless Propagation Letters***, Vol. 18, No. 3, (2019), 517-520. doi: 10.1109/LAWP.2019.2895618.
23. Asmeida, A., Abidin, Z.Z., Mohd Shah, S., Kamarudin, M.R., Malek, N.A. and Nebhen, J., "Wideband crescent-shaped slotted printed antenna with radiant circular polarisation", ***International Journal of Antennas and Propagation***, Vol. 2021, (2021), 1-12. https://doi.org/10.1155/2021/9975679
24. Hussain, M., Naqvi, S.I., Awan, W.A., Ali, W.A.E., Ali, E.M., Khan, S. and Alibakhshikenari, M., "Simple wideband extended aperture antenna-inspired circular patch for v-band communication systems", ***AEU-International Journal of Electronics and Communications***, Vol. 144, (2022), 154061. https://doi.org/10.1016/j.aeue.2021.154061
25. Koma'rudin, N., Zakaria, Z., Althuwayb, A., Lago, H., Alsariera, H., Nornikman, H., Al-Gburi, A. and Soh, P., "Directional wideband wearable antenna with circular parasitic element for microwave imaging applications", (2022). https://doi.org/10.32604/cmc.2022.024782
26. Studio, C., "Cst studio suite 3d em simulation and analysis software", ***CST Studio Suite***, (2018).
27. Balanis, C.A., "Antenna theory: Analysis and design, John wiley & sons, (2016).
28. Collin, R.E., "Foundations for microwave engineering, John Wiley & Sons, (2007).
29. Kumar, G. and Ray, K.P., "Broadband microstrip antennas, Artech house, (2002).

Persian Abstract

چکیده

طراحی یک آنتن الگوی دو طرفه باند پهن، که با ادغام یک پچ دایره‌ای، هلال‌ها به‌عنوان عناصر انگلی، احاطه‌شده توسط یک حلقه دایره‌ای مجاور سطح زمین، برای کار بری روی برنامه‌های باند متوسط G۵ زیر ٦ گیگاهرتز، انجام می‌شود. با مسی که بر روی بستر FR4 با گذردهی نسبی ٤.٣ و ارتفاع ١.٦ میلی متر طراحی و ساخته شده است. آنتن پیشنهادی توسط یک موج بر همسطح ۵۰ اهم تغذیه می شود که در همان سمت وصله دایره ای تابشی چاپ شده است. یک مدل آنتن مختصر با ابعاد ٤٥ × ٤٥ × ٠.٦ میلی‌متر مکعب ساخته شد و برای تأیید نتایج شبیه‌سازی مورد بررسی قرار گرفت. سازگاری خوب بین نتایج تجربی و شبیه سازی تایید شد. آنتن پیشنهادی از مزایای الگوی دوطرفه با بهره خوب ۵.٢٤ dBi و پوشش پهنای باند گسترده ١١١.٤٪ (١.٨١–٦.٣٦ گیگاهرتز) برخوردار است – این یکی از پیشنهادهای خوب برای کاربرد تابش جدید G۵ به ویژه برای محیط داخلی، باریک و طولانی است. منطقه خدمات مسیر مانند راهرو، تونل و ایستگاه قطار و غیره.